

## Experiment Report Form



	<b>Experiment title:</b> Temperature and composition induced transitions of pentlandite phases in Fe–Ni–Cu–S– <i>PGE</i> system	<b>Experiment number:</b> ES-699
<b>Beamline:</b> ID22	<b>Date of experiment:</b> from:30.03.2018                      to:03.04.2018	<b>Date of report:</b> 05.07.2018
<b>Shifts:</b> 12	<b>Local contact(s):</b> Andy Fitch	<i>Received at ESRF:</i>
<b>Names and affiliations of applicants</b> (* indicates experimentalists, + indicates proposers): */+ Dr. Elena Sinyakova (1), */+ Dr. Vladislav Komarov (2,3), */+ Dr. Alexander Kurnosov (4), * Dr. Taisiya Sukhikh (2,3); * Bc. student Nataliya Chuklina (3); * Bc. student Aleksandr Kurchev (3); (1) Sobolev Institute of Geology and Mineralogy SB RAS / Novosibirsk, Russia; (2) Nikolaev Institute of Inorganic Chemistry SB RAS/ Novosibirsk, Russia; (3) Novosibirsk State University / Novosibirsk, Russia; (4) Bayerisches Geoinstitut, University of Bayreuth / Bayreuth, Germany		

**Introduction.** Pentlandite with the idealized formula  $(\text{Fe}_z\text{Ni}_{1-z})_9\text{S}_8$  is one of the main nickel-rich minerals of copper-nickel ores. Natural minerals contain an admixture of copper. Pentlandite is one of the main concentrators of elements of the platinum group (*PGE*). Two morphological modifications of pentlandite (isometric and lamellar), which are in association with different sulfide minerals are described in the geological literature. It is assumed that they can crystallize from the sulfide melt, or they are the products of the solid-phase decomposition of previously crystallized minerals.

In traditional experiments, pentlandite is usually synthesized by prolonged annealing and subsequent quenching of samples [e.g., 1-3]. To simulate the formation of magmatic *PGE*–Cu–Ni–sulfide ores the directional crystallization of the sulfide melt composition (in mole %): Fe 18.5, Ni 19.1, Cu 16.7, S 44.1, Pt, Pd, Rh, Ir, Ru, Ag, Au and Te by 0.2 each element was carried out [4, 5]. As a result of crystallization, a cylindrical ingot consisting of six zones with different chemical and phase composition was obtained. This zonality is characteristic of bornite-pentlandite ore bodies. Scheme of the ingot (hereinafter referred to as *Cu2*), characteristic microstructures of the zones and the curve of the change in the total Fe content in the solid ingot and melt are shown in Fig. 1. In each zone there are grains of bornite solid solution ( $bnss = \text{Cu}_{5\pm x}\text{Fe}_{1\pm x}\text{S}_4$ ) and nickel-rich pentlandite ( $npr = (\text{Ni}_z\text{Fe}_{1-z})_9\text{S}_8$ ) with *PGE* (Pd, Rh, Ru and Ir).

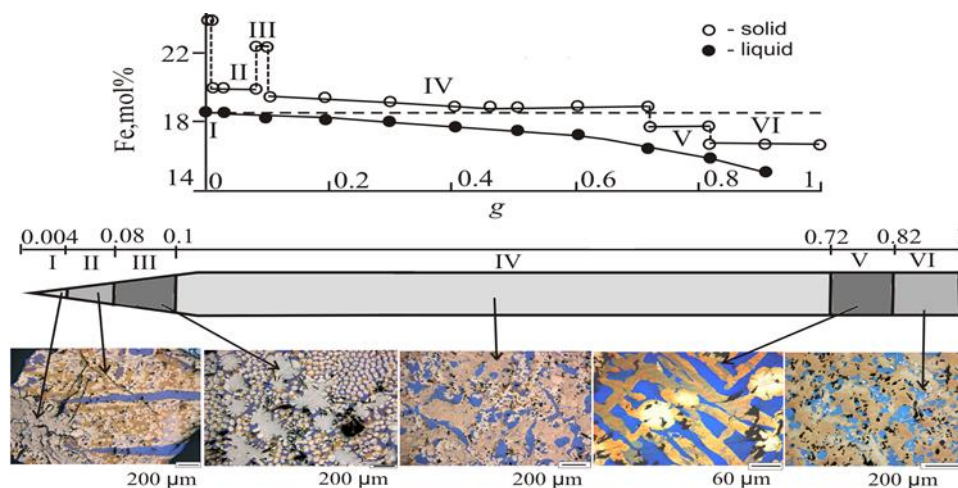


Figure 1. A scheme of a crystallized ingot, microstructure of the samples from different zones, and a curve for changing the Fe concentration in a solid ingot (open circles) and in a melt (closed circles), depending on the fraction of the crystallized melt  $g$  [4, 5].

The phase diagram of the Fe–Ni–Cu–S system in the examined composition region has been poorly studied. A study of the chemical and phase composition of this sample [4, 5] revealed three types of high-temperature pentlandite (*cfpn*, *cnpn*, *npn*), differing in cation composition, decay mechanisms, and the ability to concentrate *PGE*. While cooling, these types of pentlandites partially or completely decompose into finely dispersed low-temperature phases, among which there are two types of low-temperature copper-poor pentlandite, one of which concentrates Pd (*npn'*) and the second Pd, Rh, Ru and Ir (*npn''*). The whole set of data allows us to apprehend the existence of a complex series of solid-phase transformations through several intermediate phases, the study of which is possible only with the use of in situ methods.

However, the identification of phases by chemical composition at room temperature is not sufficient to understand the processes of phase formation and their transformations during the change of temperature. Therefore, the aim of the work is the structure identification of the samples obtained, studying the dependence of a crystal structure on the temperature, and determining the possible equations of phase reactions when the samples are heated and cooled. To achieve this goal, we fulfilled the in situ studies by powder synchrotron radiation diffraction of the samples from the IV, V and VI zones.

### The experimental procedure for directional crystallization

The initial sample (cylinder  $\text{Ø } 8.2 \times 70$  mm, Fig. 1) was obtained by directional crystallization of sulfide melt of a given composition using the vertical Bridgman method. A set of pentlandite-containing samples was obtained by transverse cutting of the original ingot. The zonal structure was determined on polished sections, studied by optical and SEM / EDX / EPMA methods and by house powder and partially single crystal XRD [4, 5].

### Method for measuring and processing diffraction patterns

In the course of the experiment, powder diffraction patterns of high resolution were measured from the samples obtained by grinding the samples taken along the length of the ingots obtained by directional crystallization. The most detailed investigation was made of the ingot *Cu2* (figure 1), for which the samples *Cu2-6* (the beginning of zone IV), *Cu2-8* (the end of zone IV), *Cu2-10* (zone V), *Cu2-12* (zone VI) were studied.

Glass capillaries 0.7 mm in diameter were used for the preparation of the samples and quartz glass was taken for high-temperature experiments. Powder diffraction patterns were measured on rotating capillaries in the range of angles  $2\theta$  0.5–28.0° of three types: (1) with "ordinary" and (2) high accumulation at room temperature (295K, 15 s/° and 120 s/°, respectively); (3) temperature movies in the high temperature range (hot air blower, 50–970–50°C, 3 s/°); (4) temperature movies in the low

temperature range (CryoStream, 20–970–50°C, 3 s/°). The temperature film parameters used made it possible to measure single diffraction patterns in approximately a 10-degree temperature range.

For *Cu2*, X-ray diffraction patterns were also measured from local regions with a size of 0.5×0.5 mm of monolithic (unmilled) "slices" of zones I-III, as preparation of samples in capillaries was impossible because of their small amount.

The indexing and the phase analysis of the diffraction patterns were carried out using the program Topas Academic v.6. Appropriate structural models of known low and intermediate temperature phases obtained from ICSD v.4.0.1 (release 2018.1) database were used in the Rietveld refinement. In cases where suitable models could not be found in the ICSD (high-temperature phases), the indexing and further Pauli refinement of the unit cell parameters (UCPs) was carried out.

### Description of the phase composition of the samples according to ES699

On the diffraction patterns of the studied samples, it is possible to distinguish two main types of sulfide phases: bornite and pentlandite. In some cases, there are also phases of the chalcopyrite group, but their peaks are sufficiently strongly masked by the bornite peaks. The obtained series of diffraction patterns with temperature change (temperature movie) made it possible to make a more reliable separation of the peaks into groups belonging to phase or several phases close in structure and composition. All phases were divided into two groups: sulfide and metal. For sulfide phases (**A–I**), a strong UCPs change from temperature is characteristic, while UCPs of metal phases (**J–N**) vary slightly. For some sulfide phases, an anomalous change in the UCPs from temperature was observed. This can be explained by a change in the chemical composition of the phases as a result of the exchange of components. Temperature regions with different temperature dependences of UCPs are indicated by numeric indices (for example, **F<sub>1</sub>–F<sub>3</sub>**). In addition, there is a background rises on all diffraction patterns above a certain temperature, which can be related to the appearance of a liquid.

Figures 2 and 3 show (2θ–T) diffraction patterns for a series of *Cu2* samples. The diffraction pattern for zone V, denoted by *Cu2-10* (Figures 2c and 3c), has the simplest form. Figures 2e and 3e depict the correlation of observable reflections to the phases. The schemes are supplemented by the position of weak peaks from the metal phases, taking into account peaks in other diffraction pattern. According to these data, a scheme of phase transformations, common for zones IV-VI (the temperatures are indicated within 10°C) is constructed. It corresponds to the following sequence of events.

- At room temperature, the basic sulfide phases are pentlandites (**A** and **B**) and orthorhombic (low-temperature) bornite (**C**). A certain number of chalcopyrite phases are masked by reflections of bornite. When heated, the UCPs of these phases increase.
- Reflections of bornite **C** disappear in the temperature range of 100–140°C, and reflections of cubic (intermediate) bornite (**D**) appear. At the same time, reflections from chalcopyrite phases disappear.
- Reflections of bornite **D** disappear in the temperature range of 200–250°C, and reflections of cubic (high-temperature) bornite (**E<sub>1</sub>**) appear.
- At ~ 220°C there appear reflections of the cubic phase (**F<sub>1</sub>**), which could not be referred to a specific mineral type.
- Up to ~ 440°C, the UCPs of phases **E<sub>1</sub>** and **F<sub>1</sub>** increase almost linearly. After this temperature, the dependence of UCPs on temperature (T) changes to anomalous – weak compression for **E** (section **E<sub>2</sub>**) and strong, accelerating with increasing temperature, for **F** (section **F<sub>2</sub>**).
- At 550°C, the appearance of a liquid is recorded and the phase **A** reflections disappear; and at 630°C the main reflections of the phase **B** disappear. After the disappearance of these phases, residual reflections (**A<sub>2</sub>** and **B<sub>2</sub>**) appear. These reflections disappear at ~ 660°C. In the region of their existence, the UCPs sharply decrease with increasing temperature.
- At 550°C and 630°C, the character of the change in the UCPs (T) for phases **E** and **F** changes. For phase **E**, strong accelerating compression (section **E<sub>3</sub>**) is observed, and for **F** – accelerating expansion (**F<sub>3</sub>**).
- At 610°C reflections appear in the new high-temperature trigonal or hexagonal phase **G**.

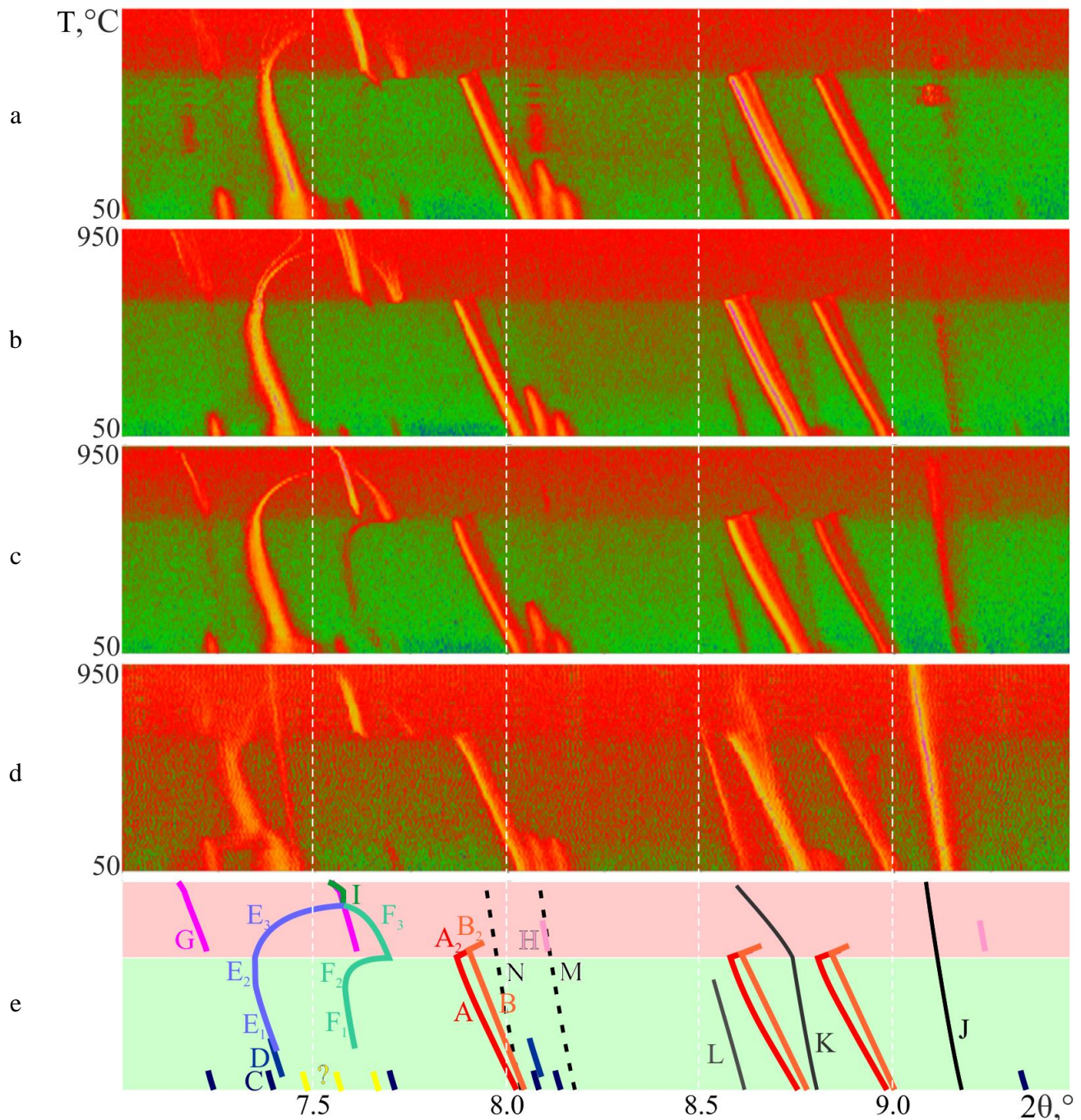


Figure 2. Map projection of temperature series of  $2\theta$  7.0–9.5° diffraction patterns of (a) *Cu2-6* and (b) *Cu2-8* (zone IV), (c) *Cu2-10* (zone V), and (d) *Cu2-12* (zone VI) samples. Arrangement of principal reflections of sulfide phases **A–H** and metal phases **J–N** schematically shown on (e). Detailed description in the text.

- At a temperature of about 630°C, a series of **H** reflections appear, gradually disappearing at 750°C. These series of reflexes can be attributed either to one phase of low crystal system (orthorhombic or lower), or to several phases of hexagonal or cubic systems. In any case, it is not yet possible to give an unambiguous matching of this group of reflexes with known mineral types.
- At a temperature of 810°C, the reflections of the **E** and **F** phases merge into reflections of the cubic phase **I**. This apparently indicates the degeneracy of two solid solutions.
- At higher temperatures of up to 900°C, phases **I** and **G** gradually dissolve, accompanied by a decrease in UCPs.

As described above, the sulfide phases **A–E** can be reliably correlated with certain mineral types and compared with the microstructure of the phases in Fig. 1. So phase **A** can be correlated with

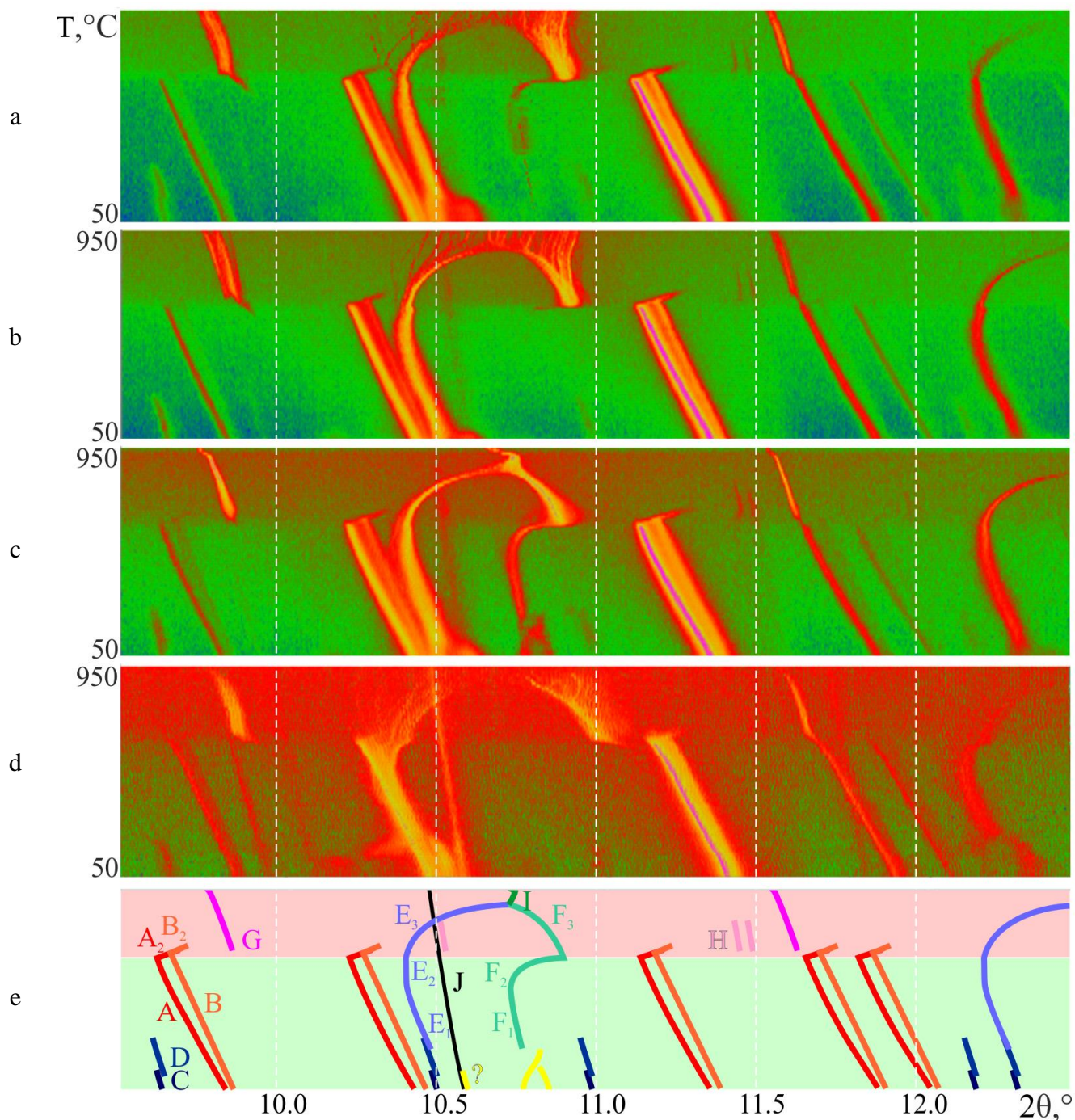


Figure 3. Map projection of temperature series of  $2\theta$  9.5–12.5° diffraction patterns of (a) *Cu2-6* and (b) *Cu2-8* (zone IV), (c) *Cu2-10* (zone V), and (d) *Cu2-12* (zove VI) samples. Arrangement of principal reflections of sulfide phases **A–H** and metal phases **J–N** schematically shown on (e). Detailed description in the text.

pentlandite *npn'*, in which only Pd dissolves. This phase was crystallized from the melt in the form of coarse grains and formed small inclusions in the solid-phase decay of high-temperature minerals. Phase **B** can be attributed to pentlandite *npn''*, in which all *PGE* are co-dissolved. The **C**, **D**, and **E** phases are close to bornites composition. Large crystals of bornite were formed directly from the melt, and the finely dispersed phases are products of solid-phase reactions. For a more detailed understanding of the processes which take place in the investigated samples, a careful structural study of the high-temperature phases **E<sub>3</sub>** and **F<sub>3</sub>** is of interest, especially the structure of the cation sublattice as a function of temperature and composition, as well as the structure and composition of **G–I** phases.

Besides sulfide phases, up to five different metal phase **J–N** with a relatively weak dependence of UCPs on *T* are detected in the samples. All these phases can be pre-assigned to cubic system. However,

Table 1. Proposed Bravais types and unit cell parameters of major phases of *Cu2-10* sample (zone V) at selected temperatures. Uncertainties of refined UCPs estimated as a few of  $10^{-3}\text{\AA}$ .

phase symbol	Bravaice type	UCPs, $\text{\AA}$ (pp#, T, $^{\circ}\text{C}$ )
<b>A</b>	<i>cF</i>	<i>a</i> 10.130 (50); 10.211 (250); 10.330 (590)
<b>B</b>	<i>cF</i>	<i>a</i> 10.100 (50); 10.166 (250); 10.280 (590)
<b>C</b>	<i>oP</i>	<i>a</i> 10.96*, <i>b</i> 21.95*, <i>c</i> 10.92* (50)
<b>D</b>	<i>cF</i>	<i>a</i> 10.955 (110); 10.978 (205)
<b>E</b>	<i>cF</i>	<i>a</i> 5.500 (250); 5.528 (590); 5.518 (660); 5.364 (825)
<b>F</b>	<i>cF</i>	<i>a</i> 5.293 (660); 5.350 (825)
<b>G</b>	<i>hP</i>	<i>a</i> 3.503, <i>c</i> 5.634 (660); 3.527, 5.696 (895)
<b>I</b>	<i>cF</i>	<i>a</i> 5.359 (850); 5.385 (895)
<b>J</b>	<i>cP</i>	<i>a</i> 3.841* (50); 3.862 (590); 3.873 (840)

\* manual UCP refinement or ICSD values.

this assignment is reliable only for phases **J** (izoferroplatinum) and **L** (gold and silver). It is interesting that the intensity of the phase **L** reflections is greatly reduced already at temperatures above  $250^{\circ}\text{C}$  and these reflections substantially vanish before the appearance of perceptible amounts of liquid phase. For the **K** phase, in contrast to the rest of the metal phases, there is a sharp change to increase of UCPs with the appearance of a liquid phase.

It should be stressed that the fractures in the dependence of UCPs on T of sulfide (**E**, **F**) and metal (**K**) phases are most likely associated with the processes of exchange of components with the surrounding phases. The change of the sections **E<sub>2</sub>–E<sub>3</sub>**, **F<sub>2</sub>–F<sub>3</sub>** and **K–K<sub>2</sub>** can be associated with a high degree of confidence in the active exchange of components with the appeared liquid phase. The causes of the breaks of **E<sub>1</sub>–E<sub>2</sub>** and **F<sub>1</sub>–F<sub>2</sub>** are not so obvious and can indicate both the appearance of a small amount of a liquid phase, undetectable *via*. XRD, or an increase in the solid-phase exchange of components in highly dispersed phases.

Presumptive structural types and UCPs of **A–N** phases in sample *Cu2-10* (zone V) at key temperatures are given in Table 1.

The main differences between the diffraction patterns of samples from zones IV and VI are as follows:

- For the sample *Cu2-6*, additional reflexes are observed in the temperature range of  $250\text{--}550^{\circ}\text{C}$ . This may indicate the formation of additional intermediate phases in the region of the onset of melting, or (which is less likely) the presence of a number of complex structural distortions (modulations) of existing sulfide phases.
- In samples *Cu2-6* and *Cu2-12*, and partly in *Cu2-8*, low-temperature sections of the reflections corresponding to phase **F** are absent. This may be due to the presence of several mechanisms of phase transformations determined by the microstructure of the sample.
- The absence of splitting of the reflections of group **G** in the sample *Cu2-8* and its presence in the remaining samples may indicate, in analogy with pentlandites **A** and **B**, the presence of two trigonal (hexagonal) high-temperature phases with different compositions of these phases in zone IV and in zones V and VI.
- There is an abrupt change in the UCPs of one of the pentlandites (**B**), bornites (**C** and **E**, as well as the almost complete absence of the **D** region) and isoferroplatinum (**J** with a significant increase in its content) in zone VI of the ingot compared to the previous zones. This indicates a sharp change in the composition of the melt in the last stages of crystallization of the ingot.
- The most mysterious is the presence of multiple splitting of peaks of sections **E<sub>3</sub>** and **F<sub>3</sub>** observed on all samples except *Cu2-10*. Such a splitting can indicate either lowering in the symmetry of high-temperature cubic phases depending on the macro- and micro-component composition of the

surrounding liquid, and on the possibility of selective absorption of components from the liquid, or formation of a large number of high-symmetry phases with differing UCPs.

- The reasons for the observed broadening of the diffraction peaks for sulfide phases at room temperature also require an explanation. Experiments to scan the initial zones I, II and III of the ingot, carried out without swinging the sample, showed that the original (not powdered) samples are significantly textured and do not have such a strong peak broadening. Therefore, the broadening can be related to the presence of composition gradients in the phases under study. They are due to the features of the formation of phases from the melt and their formation during solid-phase processes when the sample is cooled.

The investigations carried out showed that when heating a directed crystallized sample, various processes take place followed by strong changes in the volume of phases, changes in the slope of the UCPs dependences on T, and other effects. These results are the basis for a more detailed understanding of the processes of mineral formation during the formation of ore bodies as a result of fractional crystallization of multicomponent sulfide melts.

## Summary

1. A structural confirmation of the existence of two modifications of pentlandite with *PGE* impurities is obtained. Previously, these modifications were identified only by their chemical composition.
2. Important information was obtained on the behavior of sulfide and metal phases during heating and cooling of a directed crystallized sample in the Cu–Fe–Ni–S–(*PGE*, Au, Ag, Te) system, whose composition corresponds to the composition of real bornite-pentlandite ores of the Noril'sk deposits.
3. The change in unit cell parameters of sulfide and metal minerals present in the sample is determined, as well as the presence of kinks on the UCP–T dependencies was detected.
4. A generalized temperature scheme is constructed reflecting the regions of existence of different phases. It will be used for a deeper interpretation of the processes of phase formation during direct crystallization of the melts and subsequent cooling of the crystallized substance.
5. The use in situ studies by powder synchrotron X-ray diffraction made it possible to obtain unique results on the phase formation processes in the 12-component geochemical system Fe–Ni–Cu–S–(Pt, Pd, Rh, Ir, Ru, Ag, Au, Te) during fractional crystallization of the magmatic melt and to formulate the main directions for further crystal-structural studies.
6. The developed technique for studying the processes of fractional crystallization of sulfide melts using the in situ method by powder synchrotron radiation is supposed to be used for experimental modeling of the processes of formation of copper-nickel ores and the concomitant processes of concentration of *PGE*, Au and Ag in different minerals.
7. The results obtained will be used to refine the structure of the phase diagram of the basic geochemical system Cu–Fe–Ni–S.

## References

- [1] Craig, Kullerud (1969): *Econ. Geol. Monograph*. **4** 344;
- [2] Hill (1984) Sulfide deposits in mafic and ultramafic rocks. Ed. D.I. Buchmen, and M.J. Jones. 14.
- [3] Peregoedova et al. (1995): *Russ. Geol. Geophys.* **36** 91;
- [4] Kosyakov, Sinyakova (2017): *Russ. Geol. Geophys.* **58** 1520;
- [5] Sinyakova et al. (2018): *Russ. Geol. Geophys.* (*in Press*).